Available online at www.sciencedirect.com
ScienceDirect
Diamond & Related Materials 15 (2006) 1849–1854
DIAMOND AND RELATED MATERIALS
www.elsevier.com/locate/diamond

One-step growth process of carbon nanofiber bundle-ended nanocone structure by microwave plasma chemical vapor deposition

I.J. Teng, P.K. Chuang, C.T. Kuo *

Department of Materials Science and Engineering, National Chiao Tung University, Hsinchu, Taiwan

Available online 3 November 2006

Abstract

In this work, we report a simple one-step growth process to synthesize a novel and distinct carbon nanostructure, called a carbon nanofiber bundle-ended nanocone (CNFNC) structure, by using microwave plasma chemical vapor deposition (MPCVD) method with CH_4 and H_2 as source gases and Fe catalyst. The nanostructures and their properties after each processing step were characterized by FESEM, HRTEM, ED, AES, and Raman spectroscopy. The preliminary results have demonstrated that the CNFNC structures exhibit excellent field emission properties. The results also show that the favored conditions to form the CNFNC structures include a combination of lower CH_4/H_2 flow ratio, higher substrate negative bias, and proper working pressure and deposition time. The possible growth mechanism of the CNFNC structures is proposed.

Keywords: Carbon nanofibers (CNFs); Carbon nanocones (CNCs); Microwave plasma chemical vapor deposition (MPCVD); Field emission; Growth mechanism

1. Introduction

In recent years, the syntheses of various carbon nanostructures for different applications have attracted much interest in academic and technology communities, because of their unique physical and chemical properties. Possible applications include field emission display (FED) devices [1,2] and tips for scanning probe microscopy [3,4]. The main reported carbon nanostructures include carbon nanocones (CNCs) [5–7], carbon nanofibers (CNFs) [8–10], carbon nanotubes [11–13], etc. There are many processes to be developed to improve the properties or to examine their growth mechanisms, such as synthesis of CNCs on Si wafer with electron conductive layers (Pt/Ti) [14], comparing the structures and properties of CNCs synthesized on Mo or SiO_2/Si substrates by bias-enhanced MPCVD [15], developing a two-step process to synthesize cone-shaped CNF bundles [16], etc. These carbon nanostructures can exhibit outstanding field emission properties due to their higher aspect ratios and controllable number density on the substrate. However, there is still room to improve their performances, such as uniformity, adhesion with the substrate, emission stability, effective emission ability, simplicity of the process, etc.

Here, we develop a simple one-step process to synthesize a novel carbon nanostructure, being called a carbon nanofiber bundle-ended nanocone (CNFNC) structure, by MPCVD on Si substrates with Fe film as catalyst. These unique, uniformly distributed, and well-aligned CNFNC structures were proved to possess excellent field emission properties. The possible growth mechanism is proposed.

2. Experimental

The p-type Si (100) wafer substrates for nanostructures deposition were first deposited with 10 nm thick Fe film to act as catalyst by physical vapor deposition (PVD). The Fe-coated substrates were then followed by H-plasma pretreatment under 100 sccm H_2 for 10 min to obtain well-distributed nanoparticles of catalysts. The nanostructures were then grown on the pretreated substrates in a MPCVD system under different deposition times (1–40 min), working pressures (9–30 Torr), substrate biases (0 to −320 V), and CH_4/H_2 flow ratios (1/100–100/100 sccm/sccm). The specimen designations and their deposition conditions are shown in Table 1.

The substrates and the nanostructures in each processing step were characterized by field emission scanning electron microscopy (FESEM) and high-resolution transmission electron microscopy (TEM and HRTEM). The crystal and bonding structures

* Corresponding author.
E-mail address: ctkuo@mail.nctu.edu.tw (C.T. Kuo).

0925-9635/$ - see front matter © 2006 Elsevier B.V. All rights reserved.
doi:10.1016/j.diamond.2006.07.011

Table 1
The specimen designations and their deposition conditions

Specimen designation[a]	CH_4/H_2 (sccm/sccm)	Dep. time (min)	Working pressure (Torr)	Subs. bias (V)	$I(D)/I(G)$
A1	1/100	1	9	−320	N/A
A2	1/100	5	9	−320	1.75
A3	1/100	20	9	−320	0.72
A4	1/100	40	9	−320	2.10
B1	1/100	20	23	−320	0.86
B2	1/100	20	30	−320	1.58
C1	1/100	10	9	−100	1.89
C2	1/100	10	9	−200	1.01
C3	1/100	10	9	−320	0.76
C4	1/100	60	9	−100	1.64
D1	10/100	10	9	−320	1.76
D2	30/100	10	9	−320	1.49

[a] H-plasma pretreatment conditions: substrates = 10 nm thick Fe-coated Si [(100) p-type] wafers, H_2 = 100 sccm, microwave power = 400 W, and process time = 10 min.

of the nanostructures were examined by electron diffraction (ED) and micro-Raman spectroscopy with 514.5 nm laser. The Auger electron spectroscopy (AES) was used for chemical analyses of the nanostructures.

3. Results and discussion

3.1. Effects of process parameters on nanostructures

The effect of deposition time on the SEM morphologies of the as-deposited nanostructures on Fe-coated Si substrates for Specimens A1 to A4 in Table 1 is shown in Fig. 1(a) to (d) for deposition times 1, 5, 20, and 40 min, respectively. It shows the progress of conical nanostructures formation, where the average length and base diameter of the cones increase with the deposition time. It is also noted that a bundle-shape of nanostructures on the tips of the nanocones appears after 5 min deposition time; and the bundles become more obvious, well-aligned, and denser in number densities after 20 min deposition time. However, by extending the deposition time to 40 min, most of the bundles and the underneath cones are gradually damaged; they seem to be seriously etched by the plasma. In order to examine the conical nanostructures with the bundles on the tips more closely, the HRTEM lattice image of the cone-shape part of the nanostructures after removing from the substrate by ultrasonic agitation is shown in Fig. 2(a), where the inset is the corresponding ED pattern. It shows that the cone-shape part of the nanostructures is made of microcrystalline graphene walls, as also verified by its ED pattern. In other words, the cone-shape part can be called as carbon nanocones (CNCs). In contrast, the HRTEM lattice image of the individual fiber in the bundle-shape part of the nanostructures is shown in Fig. 2(b). It indicates that the tip-growth nanostructure with catalyst particle on the tip of a V-shape cavity formed by graphene layers around the axis of the fiber. It is similar to the reported herringbone carbon nanofiber (CNF) structures [17]. Furthermore, we may name the special nanostructures as carbon nanofiber bundle-ended nanocone (CNFNC) structures.

The influence of working pressure on the CNFNC structures was explored by varying the working pressures from 9 to 30 Torr under the same CH_4/H_2 ratio (=1/100 sccm/sccm) and deposition time (20 min), as depicted in the typical SEM morphologies in Figs. 1(c), 3(a), and (b) for the working pressures 9, 23 and 30 Torr, respectively (Specimens A3, B1, and B2 in Table 1).

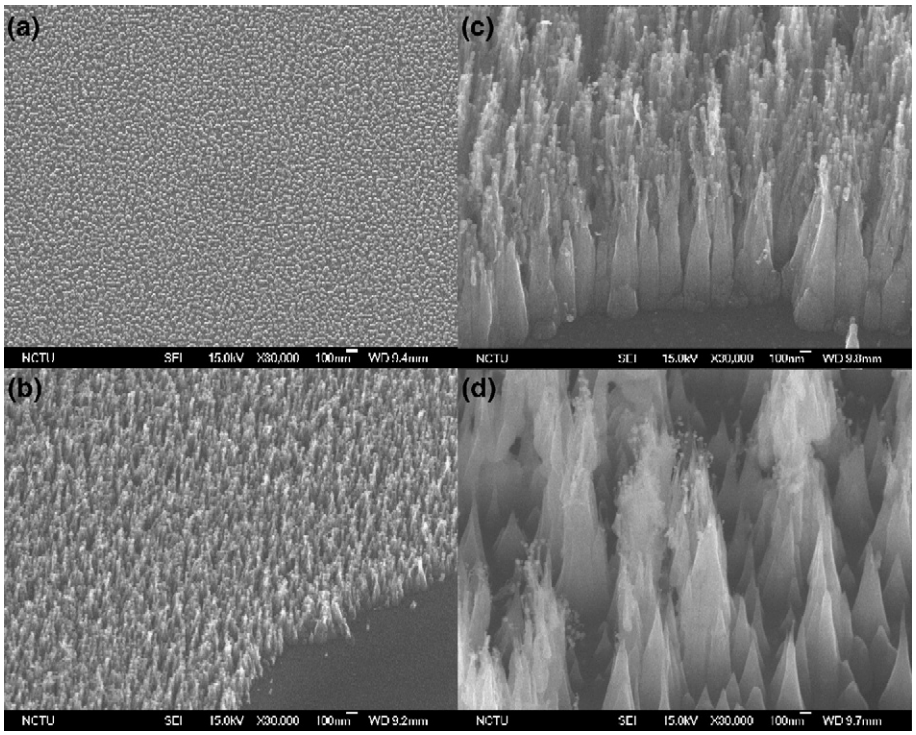

Fig. 1. Typical SEM morphologies of the nanostructures synthesized under different deposition times: (a) 1, (b) 5, (c) 20, and (d) 40 min, respectively.

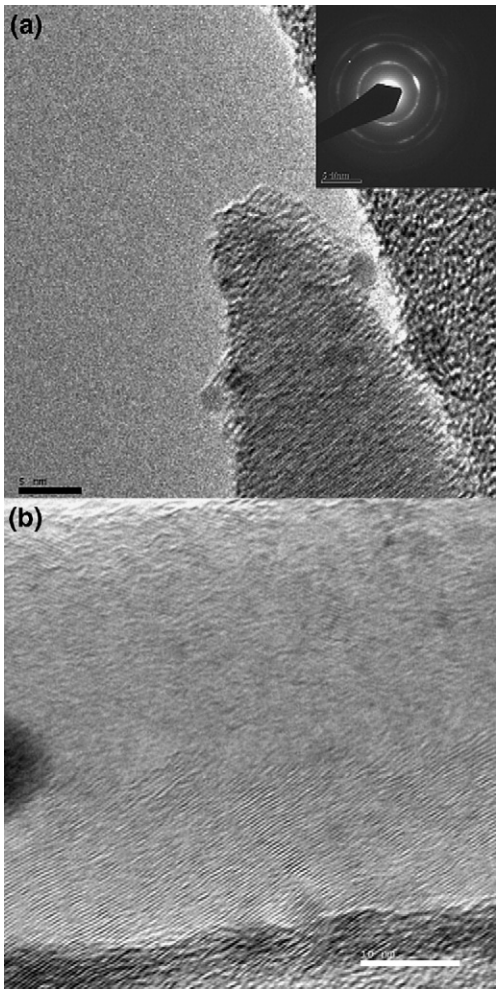

Fig. 2. HRTEM lattice images and its ED pattern of two parts of the CNFNC structures: (a) cone-shape part and (b) one fiber of the bundle-shape part.

It appears that the length ratio (= LR) of the CNF to CNC shows a maximum value (about 3.6) at 23 Torr.

The effect of the substrate bias on the CNFNC structures formation was examined at different substrate biases from 0 to −320 V. The typical SEM morphologies are shown in Fig. 4(a) to (d) for the substrate biases −100, −200, and −320 V of 10 min deposition time and −100 V of 60 min deposition time, respectively (Specimens C1 to C4 in Table 1). The results show that there is no CNFNC structures formation for substrate bias less than −100 V, even by prolonging the deposition time to 60 min, as shown in Fig. 4(d). In other words, a substrate bias greater than −200 V is one of the required conditions to form the CNF NC structures.

The effect of CH_4/H_2 flow ratio on the CNFNC structures formation was studied by varying the flow ratios from 1/100 to 100/100 sccm/sccm while keeping the deposition time, working pressure, and substrate bias at 10 min, 9 Torr, and −320 V, respectively. Variations of the SEM morphologies with different CH_4/H_2 flow ratios are presented in Figs. 4(c), 5(a), and (b) for CH_4/H_2 flow ratios 1/100, 10/100, and 30/100 sccm/sccm, respectively (Specimens C3, D1, and D2 in Table 1). It appears that the lower flow ratio (<20/100 sccm/sccm) is more favorable to form the CNFNC structures.

3.2. Raman spectra and Auger analyses of the CNFNC structures

Fig. 6 shows typical Raman spectra for the nanostructures under different deposition times. There are two peak positions of D and G bands around 1350–1355 and 1583–1600 cm^{-1}, respectively. Due to a limited penetration ability of laser power, the Raman spectra for the nanostructures around 10 to 20 min deposition times are essentially representing the Raman spectra for the CNF part of the nanostructures. In contrast, the Raman spectra at the longest (40 min) and shorter (1 to 5 min) deposition times are basically depicting the Raman spectra for the CNC part of the nanostructures, as compared to the SEM morphologies in Fig. 1 with the corresponding Raman spectra in Fig. 6. It signifies that the G peaks of the nanostructures have a tendency to shift toward 1581 cm^{-1} wave number by increasing the deposition time up to 20 min, in addition to the decrease in the $I(D)/I(G)$ ratio to a lower value (~0.72), as also shown in Table 1. In other words, the graphitization of the CNF part of the CNFNC structures is much better than the CNC part, where a lower value of $I(D)/I(G)$ ratio is an indication of better graphitization. This is also in agreement with the results on the effects of working

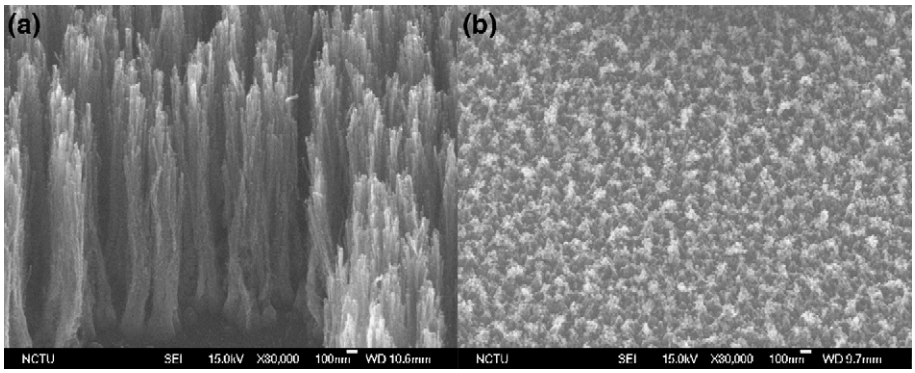

Fig. 3. Typical SEM morphologies of the CNFNC structures synthesized under different working pressures: (a) 23 and (b) 30 Torr, respectively.

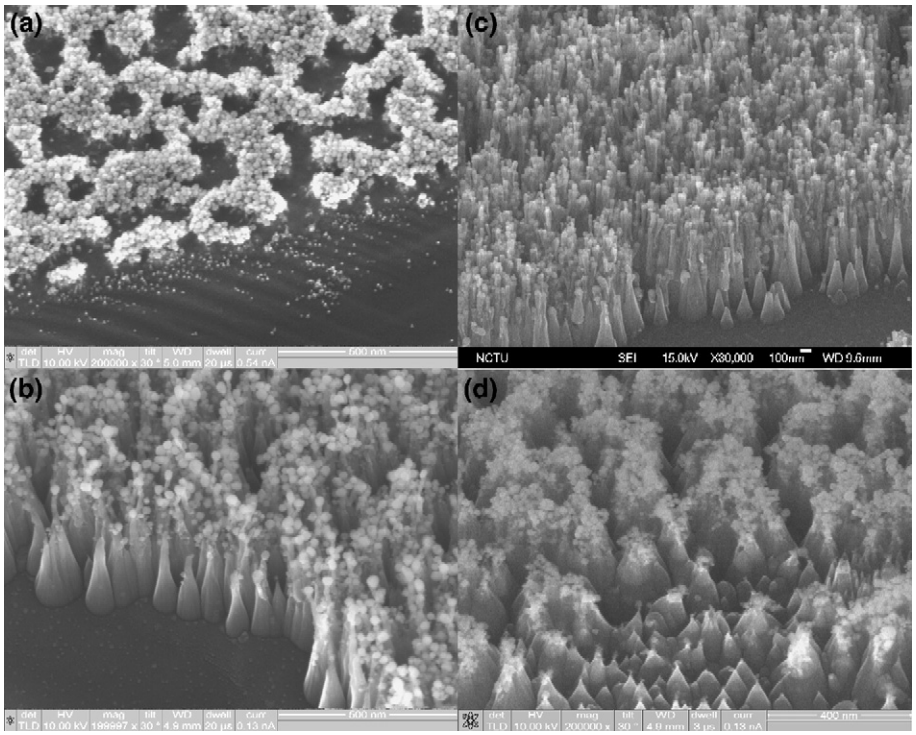

Fig. 4. Typical SEM morphologies of the CNFNC structures synthesized under different substrate biases and deposition times: (a) −100 V, (b) −200 V, and (c) −320 V for 10 min deposition time, and (d) −100 V for 60 min deposition time, respectively.

pressure, substrate bias, and CH_4/H_2 flow ratio on the morphologies of the nanostructures. The favored conditions to form the CNF part of the nanostructures are lower working pressure, higher negative substrate bias, and lower CH_4/H_2 flow ratio, which are also the favored conditions to give a lower I(D)/I(G) value or better graphitization, as shown in Table 1.

In order to examine the types of carbon structures in the CNC part, the typical AES spectrum and its magnified spectrum around carbon peaks are shown in Fig. 7(a) and (b), respectively. The signals of oxygen and nitrogen in Fig. 7(a) are believed to be due to the contamination of the specimen in air during specimen handling. By comparing Fig. 7(b) with the reported AES spectra by Lin's group [18], the features of the peaks around 252 eV and 275 eV for the CNC part are close to the reported features of the peaks around 248 eV and 271 eV for graphite with a shift of 4 eV in value due to the AES system shift. The result confirms that the CNCs may consist of graphene structures in disordered carbon matrix, as indicated in HRTEM, ED, and Raman examinations.

3.3. Our proposed growth mechanism of the CNFNC structures

The growth of the CNFNC structures is essentially consisting of the CNC growth and followed by the CNF growth on the tips of the CNCs. The proposed growth mechanisms for the CNCs formation include electrostatic force-induced cone-shape catalyst formation [15], vertical C-diffusion and lateral C-precipitation competition growth mechanism [19], and progressive decrease in catalyst size

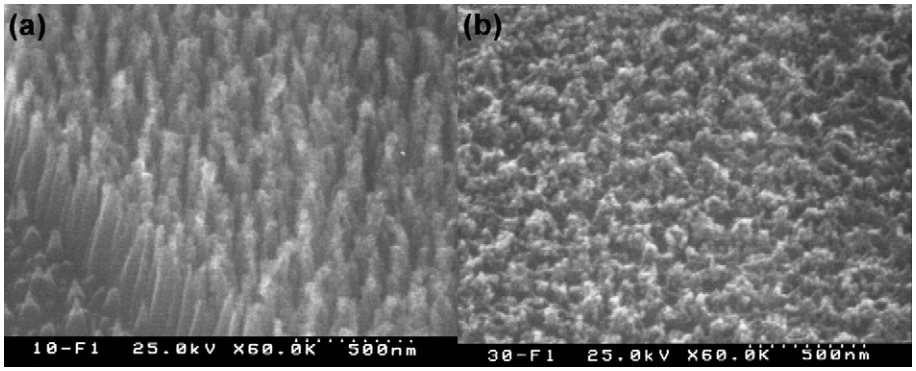

Fig. 5. Typical SEM morphologies of the CNFNC structures synthesized under different CH_4/H_2 flow ratios: (a) 10/100 and (b) 30/100 sccm/sccm, respectively.

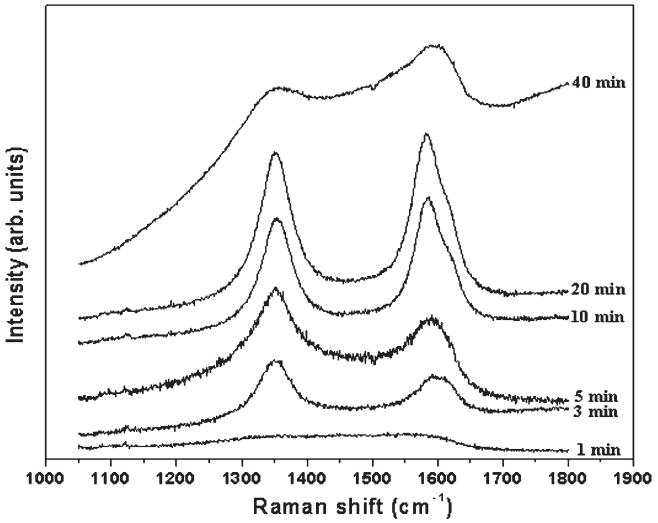

Fig. 6. Typical Raman spectrum for the nanostructures under different deposition times.

due to plasma etching [7]. We propose that the formation of the CNCs is essentially the result of a relative higher carbon deposition rate than the etching rate of carbon nanostructures, in addition to a progressive reduction in catalyst particle sizes due to plasma bombardment or etching. In other words, a higher catalyst etching rate gives rise to a shorter cone.

Here, we also propose that the possible mechanism to develop bundles of CNFs on CNCs to form CNFNC structures may be due to a strong bombardment of the positive species in the reaction atmosphere to perturb the catalyst surface to become few loosely attached extrusions, which act as catalysts to grow CNFs. In other words, the favored process conditions to form a bundled structure are the conditions which can perturb the catalyst surface more easily, such as, enough thinner or smaller catalysts which can be more easily bombarded to form much smaller separated catalysts besides the possible steps or in the cavities on the cone tip surface. This mechanism is supported by the facts that a higher reaction pressure may result in a slightly higher temperature and higher species density to cause a greater perturbation on the catalyst surface to promote formation of a bundled structure. However, if the pressure is too high, the bombardment may accelerate the etching rate of catalyst sizes and so to form shorter CNCs with less CNFs on their tips. This is why there is no CNFNC structures formation at 30 Torr reaction pressure. As discussed in the previous section, the other favored conditions to form the CNFNC structures are enough higher negative substrate bias, and lower CH_4/H_2 flow ratio. A higher enough negative substrate bias is essential to possess enough energy to cause such perturbation. A lower CH_4/H_2 flow ratio is basically the condition which shifts the balance between carbon deposition rate and catalyst etching rate to give a favorable condition to form more CNFs on CNCs.

4. Conclusions

A one-step growth process to synthesize carbon nanofiber bundle-ended nanocone (CNFNC) structures on Si wafer was successfully developed by MPCVD. By comparing with the reported values in the literature, the preliminary results show that the CNFNC structures possess excellent field emission properties with the lowest turn-on voltage (less than 0.6 V/μm at 1 mA/cm^2) and high current densities (>35 mA/cm^2 at 10 V/μm). The structure–property relationship for such CNFNC structures is prepared to be published in the near future. The possible growth mechanism to form such unique nanostructures was proposed. The mechanism can be used to explain the following favorable conditions to synthesize the CNFNC structures: a lower CH_4/H_2 flow ratio (~1/100 sccm/sccm), a higher substrate bias (>−200 V), working pressure below 23 Torr, and above 5 min deposition time. The formation of CNCs in CNFNC structures is essentially the result of a relative higher carbon deposition rate than the etching rate of carbon nanostructures, in addition to a progressive reduction in catalyst particle sizes due to plasma bombardment or etching. The formation of CNFs on CNCs is basically the result of the splitting of catalysts to form the separated catalyst droplets just enough to sit in the cavities of the CNC tip surface to grow bundle of CNFs.

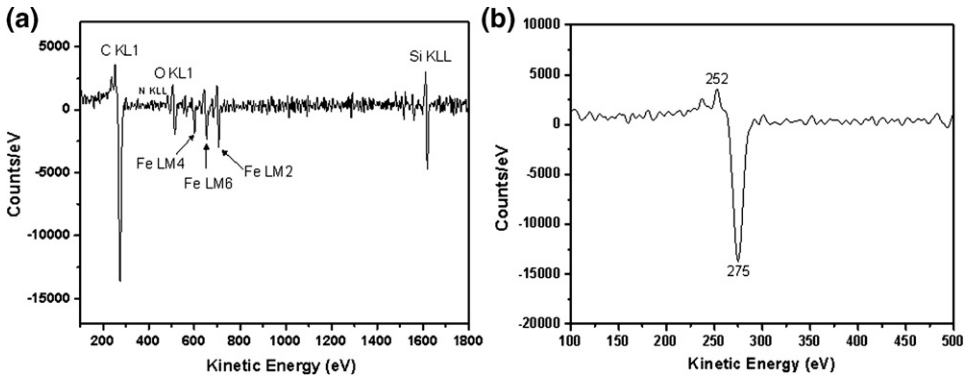

Fig. 7. Typical AES spectra of the CNC part of the CNFNC structures: (a) whole spectrum and (b) part of the magnified spectrum around carbon peaks.

Acknowledgement

This work was supported by the National Science Council of Taiwan under Contract nos. NSC 92-2120-M-009-001, NSC93-2120-M-009-003, and NSC93-2216-E-009-004.

References

[1] W.B. Choi, Y.W. Jin, H.Y. Kim, S.J. Lee, M.J. Yun, J.H. Kang, Y.S. Choi, N.S. Park, N.S. Lee, J.M. Kim, Appl. Phys. Lett. 78 (2001) 1547.
[2] S.H. Lim, H.S. Kim, J. Jang, C.H. Lee, L.S. Park, D.H. Shin, SID 02 DIGEST P-42, 2002, p. 356.
[3] V.I. Merkulov, A.V. Melechko, M.A. Guillorn, D.H. Lowndes, M.L. Simpson, Appl. Phys. Lett. 80 (2002) 4816.
[4] H. Dai, J.H. Hafner, A.G. Rinzler, D.T. Rinzler, D.T. Colbert, R.E. Smalley, Nature 384 (1996) 147.
[5] W.H. Wang, Y.T. Lin, C.T. Kuo, Diamond Relat. Mater. 14 (2005) 907.
[6] G. Zhong, T. Iwasaki, H. Kawarada, I. Ohdomari, Thin Solid Films 315 (2004) 464.
[7] L.H. Chen, J.F. AuBuchon, A. Gapin, C. Daraio, P. Bandaru, S. Jin, D.W. Kim, I.K. Yoo, C.M. Wang, Appl. Phys. Lett. 85 (2004) 5373.
[8] K.B.K. Teo, M. Chhowalla, G.A.J. Amaratunga, W.I. Milne, G. Pirio, P. Legagneux, F. Wyczisk, D. Pribat, D.G. Hasko, Appl. Phys. Lett. 80 (2002) 2011.
[9] Y. Wang, S.H. Jo, S. Chen, D.Z. Wang, Z.F. Ren, Nanotechnology 17 (2006) 501.
[10] C.T. Hsieh, J.M. Chen, R.R. Kuo, Y.H. Huang, Rev. Adv. Mater. Sci. 5 (2003) 459.
[11] W.H. Wang, Y.R. Peng, C.T. Kuo, Diamond Relat. Mater. 14 (2005) 1906.
[12] C.C. Lin, P.L. Chen, C.T. Lin, C.T. Kuo, Diamond Relat. Mater. 14 (2005) 1867.
[13] P.L. Chen, J.K. Chang, C.T. Kuo, F.M. Pan, Appl. Phys. Lett. 86 (2005) 123111.
[14] C.L. Tsai, C.F. Chen, L.K. Wu, Appl. Phys. Lett. 81 (2002) 721.
[15] Y. Hayashi, T. Tokunaga, T. Soga, T. Jimbo, Appl. Phys. Lett. 84 (2004) 2886.
[16] C.J. Huang, C.M. Yeh, M.Y. Chen, J. Hwang, C.S. Kou, J. Electrochem. Soc. 153 (1) (2006) H15.
[17] N.M. Rodriguez, A. Chambers, R.T.K. Baker, Langmuir 11 (1995) 3862.
[18] C.R. Lin, T.J. Wang, K.C. Chen, C.H. Chang, Mater. Chem. & Phys. 72 (2001) 126.
[19] V.I. Merkulov, M.A. Guillorn, D.H. Lowndes, M.L. Simpson, E. Voelkl, Appl. Phys. Lett. 79 (2001) 1178.